Conservation Biology

Bridging conservation gaps under climate change at multiple scales to protect 30% of Earth's surface by 2030

Hui Wu[1] ![ORCID] | Le Yu[1,2,3] | Xiaoli Shen[4] ![ORCID] | James E. M. Watson[5,6] | Huawei Wan[7] |
Yue Cao[8,9] | Ting Hua[10] | Tao Liu[1] | Jianqiao Zhao[11] ![ORCID] | Jianguo Liu[12] | Jixi Gao[7] |
Keping Ma[4] ![ORCID]

[1]Department of Earth System Science, Ministry of Education Key Laboratory for Earth System Modeling, Institute for Global Change Studies, Tsinghua University, Beijing, China

[2]Ministry of Education Ecological Field Station for East Asian Migratory Birds, Beijing, China

[3]Tsinghua University (Department of Earth System Science)–Xi'an Institute of Surveying and Mapping Joint Research Center for Next-Generation Smart Mapping, Beijing, China

[4]State Key Laboratory of Vegetation and Environmental Change, Institute of Botany, Chinese Academy of Sciences, Beijing, China

[5]School of the Environment, University of Queensland, St. Lucia, Queensland, Australia

[6]Centre for Biodiversity and Conservation Science, University of Queensland, St. Lucia, Queensland, Australia

[7]Center for Satellite Applications on Ecology and Environment, Ministry of Ecology and Environment, Beijing, China

[8]Institute for National Parks, Tsinghua University, Beijing, China

[9]Department of Landscape Architecture, School of Architecture, Tsinghua University, Beijing, China

[10]Industrial Ecology Programme and Department of Energy and Process Engineering, Norwegian University of Science and Technology, Trondheim, Norway

[11]College of Land Science and Technology, China Agricultural University, Beijing, China

[12]Science and Policy Program, Michigan State University, East Lansing, Michigan, USA

Correspondence
Le Yu, Department of Earth System Science, Ministry of Education Key Laboratory for Earth System Modeling, Institute for Global Change Studies, Tsinghua University, Beijing 100084, China.
Email: leyu@tsinghua.edu.cn

Article impact statement: The 30×30 commitment boosts conservation in China and Southeast Asia by addressing climate change risks and species priorities across scales.

Funding information
National Key Research and Development Program of China, Grant/Award Numbers: 2022YFE0209400, 2024YFF1307600; National Natural Science Foundation of China, Grant/Award Number: 42401314; China Postdoctoral Science Foundation, Grant/Award Number: 2023M741885; Tsinghua University Initiative Scientific Research Program, Grant/Award Number: 20223080017; the National Key Scientific and Technological Infrastructure project Earth System Science Numerical Simulator Facility (EarthLab)

Abstract

The 30×30 commitment outlined in the Kunming–Montreal Global Biodiversity Framework (KM-GBF) offers a critical opportunity for enhancing global biodiversity conservation. However, KM-GBF's efforts to address climate change impacts remain limited. We developed 1-km-resolution hotspot maps for climate change vulnerability with the exposure–sensitivity–adaptation framework, species distribution for 4 terrestrial vertebrate taxa, and carbon stock capacity including organic and biomass carbon, for 2030. Then, we developed a systematic conservation planning approach that, beyond the 3 conservation features mentioned, also considered human activities, connectivity, and Shared Socioeconomic Pathways. The plan included the identification of conservation priorities and gaps for China and the Association of Southeast Asian Nations region (China-ASEAN) at regional, national, and biogeographical scales. We found that 6.59% of the land in China-ASEAN overlapped all 3 hotspots, primarily in Indonesia, Malaysia, and Cambodia. Across all 3 spatial scales, newly identified conservation priorities were concentrated in low-elevation areas, particularly between 10° S and 10° N at the regional scale. Currently, protected areas cover 15.49% of China-ASEAN's land, representing 7.00% of climate change vulnerability hotspots, 12.45% of species distribution potential hotspots, and 14.56% of carbon stock capacity hotspots for 2030. If the 30×30 commitment is realized at a regional scale, these percentages are expected to increase to 22.93%, 33.15%, and 34.75%, respectively. Areas of conservation priority identified with our framework were significantly affected by the scale of protection coordination, yet they remained stable across Shared Socioeconomic Pathways, indicating their effectiveness in diverse future scenarios. The biogeographical scale had the smallest average conservation gap for all 12 countries (13.14%). Financial challenges are highest for Indonesia at the regional scale

Conservation Biology

and for Malaysia at the national and biogeographical scales. Precise conservation based on appropriate scales is essential to achieving the 30×30 commitment and maximizing its conservation effectiveness under climate change.

INTRODUCTION

Biodiversity loss endangers Earth's life-support systems and stands as one of the most pressing challenges confronting human society today (Bai et al., 2021; Naidoo et al., 2019). As the foundation of modern-day conservation approaches, protected areas (PAs) are critical fortresses for maintaining biodiversity and resisting human disturbance. Existing PA networks have large coverage gaps (Watson et al., 2014)—only 22.5 million km^2 (16.64%) of land and inland water ecosystems are in documented protected and conserved areas (Allan et al., 2022; UNEP-WCMC et al., 2020; Wu et al., 2023). To address these gaps, priorities for conservation of forest intactness have been identified, ecosystem restorations have been conducted, and habitat for different taxa and endangered species has been protected, for example. However, such efforts are often based on historical data and static environmental conditions, thus neglecting the crucial dynamic factor of climate change. The impacts of climate change on biodiversity and ecosystems are intricate and profound. For example, rising temperatures and increasingly frequent extreme weather events may render previously protected habitats unsuitable for species (Urban, 2015). Affected species may migrate to more climatically suitable environments that have been heavily modified by humans (Elsen et al., 2020; Wang et al., 2020). Climate change can alter the structure, composition, and function of ecosystems (Doughty, 2015), posing great risks to vulnerable ecosystems. Given the above impacts of climate change at species and ecosystem levels (Jung et al., 2021; Visconti et al., 2019), current PA networks may not be able to inadequately reduce extinction rates and prevent the degradation of critical ecosystems (Baynham-Herd et al., 2018; Dobrowski et al., 2021; Farhadinia et al., 2019).

The year 2030 marks the midterm goals for climate-specific policies in many countries, especially tropical nations. Over 190 countries have committed to protecting 30% of Earth's surface by 2030, a target known as 30×30, as outlined in the KM-GBF. Achieving this target globally is a formidable challenge that requires robust global assessments and fine-scale regional studies to build experience and enhance social acceptance (Yu et al., 2022). Efforts to integrate climate change in conservation prioritization have significantly advanced the field and have focused on particular metrics, such as climatic velocity, environmental diversity, and carbon storage, to enhance spatial resilience and ecological stability (Carroll et al., 2017; Mackey et al., 2012; Zhu et al., 2021). However, further work is needed to fully address climate change vulnerability by incorporating climate change exposure, sensitivity, and adaptation metrics in conservation prioritization. The KM-GBF has made promising strides, such as introducing the bioclimatic ecosystem resilience index (BERI) (Ferrier et al., 2020), but its overall efforts to develop climate-change-related indicators remain limited. When estimating which areas should be prioritized for protection under 30×30, how nations choose to coordinate the expansion of PAs is crucial (Sasmito et al., 2023). This coordination can be transnational or national. Global or regional coordination would optimally protect biodiversity in the broadest sense. Coordinating protection at the national level enables each contracting party to organize protection within its own borders more feasibly. The biogeographical region-based approach can significantly increase the diversity of ecosystem types in the PA network.

We selected 2030 as our target year and China and the Association of Southeast Asian Nations region (hereafter China-ASEAN region) as our research area, given its global significance in conservation (Appendix S1). This region, home to the world's most carbon-rich mangroves and 4 megadiverse countries (China, Indonesia, Malaysia, and the Philippines), serves as a vital biodiversity corridor for migration and reproduction (Carvalho et al., 2019; Mason et al., 2020). However, it faces escalating threats from forest clearance and biodiversity loss (Feng et al., 2021; Sasmito et al., 2023). For China-ASEAN, we mapped climate change vulnerability, species distribution potential, and carbon stock capacity by 2030 (i.e., conservation features). We simulated 30×30 PA expansion scenarios under varying spatial planning scales and Shared Socioeconomic Pathways (SSPs) (Figure 1). We quantified the representativeness of existing PAs in safeguarding 2030 conservation hotspots and assessed the improved representativeness achievable under the 30×30 targets. Conservation gaps and challenges faced by the 12 countries in China-ASEAN in addressing these gaps were measured. Additionally, the impact of different SSP scenarios and the spatial scale of planning on these gaps and challenges was examined. We sought to provide an integrative framework for identifying conservation priorities under future climate scenarios and insights to enhance PA networks in China-ASEAN through coordinated spatial planning.

METHODS

Climate change vulnerability

Climate change vulnerability was characterized within a widely accepted framework of climate change exposure, sensitivity, and
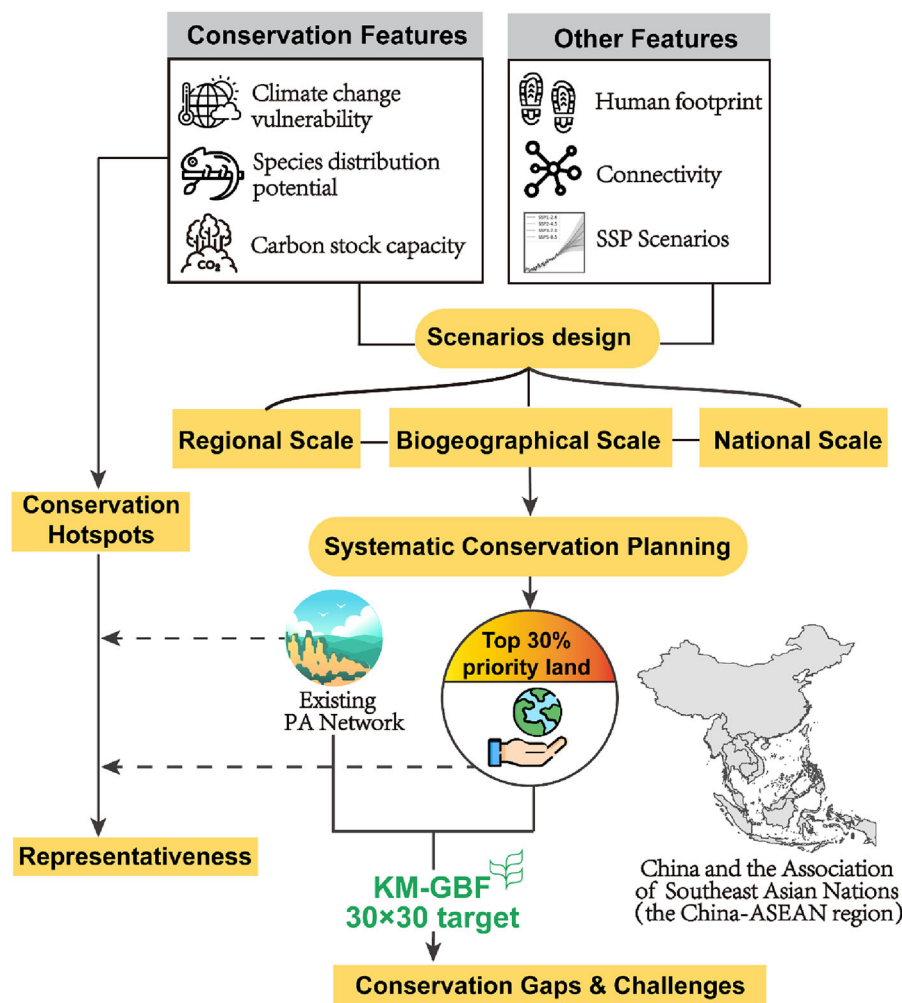
FIGURE 1 Framework of a comprehensive methodology for predicting and analyzing conservation features in China and the Association of Southeast Asian Nations (China-ASEAN) to meet the 30×30 target (30% of Earth protected by 2030) by forecasting climate change vulnerability, species distribution potential, and carbon stock capacity across regional, national, and biogeographical spatial scales under Shared Socioeconomic Pathways SSP126, SSP245, SSP370, and SSP585.

adaptation (Li et al., 2018; Ureta et al., 2022). The climate change exposure index quantifies the degree of this exposure in a given environment. Typically, climate change exposure is assessed using climate velocity, which measures the rate of shifting climate conditions across landscapes (Brito-Morales et al., 2018; Loarie et al., 2009). The climate change sensitivity index quantifies the potential for refugia or climatically stable areas to occur under climate change (Bowler et al., 2017; Jones et al., 2009). The climate change adaptation index measures environmental heterogeneity, reflecting a region's diversity of niches, facilitation of migration, or provision of ecosystem components in response to changing climate conditions (Keppel et al., 2011). These indices are designed to assess landscape-level vulnerability to climate change, rather than species-specific or biotic ecosystem vulnerabilities (Nicholson et al., 2021). They provide interpretable and actionable metrics to improve the resilience and representativeness of PAs across diverse contexts, rather than serving as inputs to a black-box prioritization model. We used Equation (1) to incorporate climate change exposure, sen-

sitivity, and adaptation in an overall climate change vulnerability (CCV) index (Ippolito et al., 2010; Li et al., 2018):

$$CCV = \sqrt{\frac{EI \times SI}{1 + AI}}, \qquad (1)$$

where CCV is the climate change vulnerability, EI is the climate change exposure index, SI is the sensitivity index, and AI is the adaptation index.

The climate change exposure index was calculated by determining the velocity of temperature and precipitation (Li et al., 2018; Michalak et al., 2020). Species undergo shifts in their distribution ranges in response to climate change. The velocity at which climate changes take place determines the required migration rate for species to adapt and stay synchronized (Carrasco et al., 2021). We computed the instantaneous velocity of climate change with the ratio of temporal and spatial gradients of mean annual near-surface temperature and annual

precipitation (Loarie et al., 2009):

$$\text{Climate velocities} = \frac{\text{Temporal gradient}}{\text{Spatial gradient}} = \frac{°C/\text{year}}{°C/\text{km}}$$

$$or\ \frac{mm/\text{year}}{mm/\text{km}} = \frac{km}{\text{year}}.$$

The temporal gradient denotes the local contrast between baseline and future climate layer values in each grid cell. We calculated gradient velocities for temperature (degrees Celsius per year) and precipitation (millimeters per year). Temperature and precipitation data were acquired from the World-Clim (https://worldclim.org/data/cmip6/cmip6climate.html) database for the baseline (1970–2000) and future (2020–2040).

To address uncertainties, we averaged outputs from 3 widely used global climate models (GCMs) (IPSL-CM6A-LR, GISS-E2-1-H, and MPI-ESM1-2-LR) across 4 SSPs (126, 245, 370, and 585). Spatial gradients were computed using future climate data in a 3×3 grid cell neighborhood and the average maximum technique (Burrows et al., 2011). We calculated temporal gradient velocities for temperature (degrees Celsius per year) and precipitation (millimeters per year). North–south gradients were derived as the variance in temperature and precipitation between northern and southern grid cell pairs, normalized by their distance. To convert cell height in latitudinal degrees to kilometers, we used a conversion factor of 111.325 km/degree. Similarly, west–east gradients were calculated for western and eastern grid cell pairs, and the conversion of cell width in longitudinal degrees to kilometers was achieved using Equation (3):

$$\text{Cell width} = \cos\left(\frac{\pi}{180}\theta\right) \times 111.325, \quad (3)$$

where cell width is in kilometers and θ is the cell width in longitudinal degrees. The average north–south and west–east gradients for the focal cell were subsequently computed. To mitigate the occurrence of flat spatial gradients that could result in infinite velocity values (Sandel, 2011), we introduced uniformly distributed random noise to each cell. The added noise ranged from −0.05 to 0.05°C for temperature and from −0.5 to 0.5 mm for precipitation (Li et al., 2018).

The sensitivity index aligns with greenspot analysis which is based on satellite data Fraction of photosynthetically Active Radiation (FPAR), identifies climatically stable microrefugia, and provides insights for global conservation planning (Mackey et al., 2012). For the sensitivity index, we used phenological observations made over 20 years or longer (Menzel et al., 2006; Reed et al., 2013; Thackeray et al., 2010). We calculated the standard deviation of the enhanced vegetation index (EVI) over 22 years (2001–2022), excluding the maximum and minimum values for each grid cell, to represent ecosystem sensitivity. We utilized the MODIS Terra Vegetation Indices product (MOD13Q1) to generate annual EVI data for 2001–2022. The MOD13Q1 provides 16-day composites of EVI at a 250-m spatial resolution. The data were sourced from the NASA LP

DAAC (Land Processes Distributed Active Archive Center) via Google Earth Engine. To derive yearly EVI values, we averaged the 16-day EVI composites for each year. This method allowed us to monitor and analyze vegetation dynamics over the specified period with high temporal consistency and spatial detail.

The adaptation index was derived from the environmental heterogeneity of the central pixel and its surrounding pixels (Zheng et al., 2023). As a key driver of adaptation potential in conservation planning (Carroll et al., 2017), environmental heterogeneity captures spatial variability in abiotic factors, such as topography and land cover. High topographic heterogeneity fosters diverse microclimates and resources that support species richness and local biodiversity, and land-cover heterogeneity enhances plant diversity and structural variation, strengthening ecosystem resilience and capacity to adapt to environmental changes (Gao et al., 2021). To quantify topographic heterogeneity, we used the ASTER Global Digital Elevation Model V003 (ASTER GDEM) at a 1-km resolution (available at https://www.earthdata.nasa.gov/). We calculated the standard deviation of elevation values in a 5 × 5-km moving window and assigned this value to the central pixel. We calculated the Shannon diversity index (H') of the central pixel with a 5 × 5-km moving window to quantify land-cover heterogeneity. We used the PFT (plant functional type)-based land projection data set under the SSPs (Chen et al., 2022). These projections cover 20 land types (19 of which exist in China-ASEAN) for 2015–2100 at a 1-km resolution. We calculated H' as follows:

$$H' = -\sum \left(p_i \times \ln p_i\right), \quad (4)$$

where p_i is the proportion of land-cover type i in the window. High spatial variability in elevation indicates the availability of diverse thermal refuge conditions in a small area (Elsen et al., 2021; Keppel et al., 2011).

Species distribution potential

To explore the conservation value of biodiversity at the pixel scale under future climate conditions, we employed the Max-Ent model (Convertino et al., 2014; Phillips et al., 2006, 2017) to project future species distribution potential. Although using species' range extent derived from the International Union for Conservation of Nature (IUCN) Red List (https://www.iucnredlist.org/en) (D'Agata & Maina, 2022) or extracting a species' area of habitat (AOH) based on habitat preferences (Shen et al., 2023) are more commonly used methods, these approaches represent only the current distribution of species and do not account for potential changes in species distribution due to climate change, which cannot be overlooked. The MaxEnt model, grounded in the principle of maximum entropy, facilitates the simulation of a species' probability distribution by incorporating known constraints, such as observation records and bioclimatic variables (Xu et al., 2017). We specifically targeted terrestrial vertebrate taxa: mammals, birds, reptiles, and

amphibians. We obtained the geographic coordinates of species distribution points for 2225 reptiles, 1611 amphibians, 2670 mammals, and 4202 birds via 2 methods. First, we collected occurrence records from PREDICTS (Hudson et al., 2017) and the Global Biodiversity Information Facility (GBIF) (https://www.gbif.org) for the 4 taxa in our research area. Second, we divided the spatial range of each species into grids to generate a series of random points. Data on the ranges of mammals and amphibians were extracted from the IUCN Red List database. Range maps for birds were sourced from BirdLife International (https://www.birdlife.org/), and information on reptiles was compiled from the IUCN and the Global Assessment of Reptile Distributions (GARD). We employed DGGRID software (Sahr, 2018) to divide China-ASEAN into 6822 equal-area hexagonal grids with the ISEA DGG (icosahedral Snyder equal-area discrete global grid). We generated a single random point in each hexagonal grid that corresponded to the species' distribution range and filtered out duplicate or erroneous records. The remaining coordinates were used as input for MaxEnt. A summary of species counts and occurrence records is in Table 1.

We retrieved 19 bioclimatic variables for 4 SSP scenarios from 3 GCMs for 2021–2040 (Appendix S2) and used them in the environmental layers for MaxEnt. To further enhance model accuracy, we also incorporated the PFT-based land projection data set (Chen et al., 2022) as an additional environmental layer. In configuring the MaxEnt model, 25% of the species occurrence points were randomly selected as test samples; the remaining 75% were used for model training. Other parameter settings included a maximum of 500 iterations, a regularization multiplier set to 1, and a cap of 10,000 background points. The MaxEnt procedure was executed with 10 bootstrap replications for each species taxon. For the distribution of each taxon under each SSP scenario, we employed the mean predictions derived from 3 GCMs to enhance robustness. Consequently, the species distribution potential at each cell was characterized by the mean distribution probabilities of all 4 vertebrate taxa. We ensured good predictive accuracy by setting a minimum area under the curve (AUC) threshold of 0.75 for model performance and evaluated models with quantitative metrics (e.g., AUC) and qualitative validation by species experts to confirm alignment with known ecological and distribution patterns.

Carbon stock capacity

The carbon sequestration capacity of the ecosystem in 2030 was assessed across China-ASEAN by integrating soil organic carbon and biomass carbon (Jung et al., 2021; Zhu et al., 2021). Vulnerable soil organic carbon, representing carbon sequestrations susceptible to potential loss over the next years due to land-use changes, was evaluated separately for mineral and organic soils. In line with the U.S. Department of Agriculture (Mulligan, 2013), organic soils were defined as those with a $\geq 5\%$ probability of being histosols, whereas other soils were categorized as mineral soils (Hengl & Wheeler, 2018).

The loss of carbon sequestration in mineral soils due to climate change was estimated at a depth of 30 cm. For organic

TABLE 1 Number of species and occurrence records by source and taxa for reptiles, amphibians, mammals, and birds in China and the Association of Southeast Asian Nations region used to map species distribution potential.

Source	Reptile Species count	Reptile Occurrence records	Amphibian Species count	Amphibian Occurrence records	Mammal Species count	Mammal Occurrence records	Bird Species count	Bird Occurrence records
PREDICTS	19	216	35	163	115	6088	706	41,431
GBIF	151	9990	1118	137,533	2305	104,613	3545	41,594
IUCN	1051	245,618	1395	111,157	1502	464,362	—	—
GARD	1103	129,458	—	—	—	—	—	—
BirdLife	—	—	—	—	—	—	3157	677,706
Total	2225	385,282	1611	248,853	2670	575,063	4202	760,731

Abbreviations: GARD, Global Assessment of Reptile Distributions; GBIF, Global Biodiversity Information Facility; IUCN, International Union for Conservation of Nature.

soils, the depth was 200 cm (Hengl & Nauman, 2019). The Intergovernmental Panel on Climate Change (IPCC) change factors (applied to mineral soils) and emission factors (applied to organic soils) were employed to estimate vulnerable soil organic carbon (kilograms per square meter) sequestrations, based on IPCC land-cover categories and climate zones.

Biomass carbon (megagrams per hectare) was estimated using the integrated valuation of ecosystem services and trade-offs (InVEST) model (Natural Capital Project, 2024). This calculation involved determining carbon content in 3 distinct pools, namely, aboveground biomass, belowground biomass, and nonliving materials. Carbon sequestration densities for each cell in the PFT-based land projection raster were computed (Chen et al., 2022; Wu et al., 2023). The InVEST carbon sequestration model's biophysical data (in Appendix S3) were developed from the IPCC lookup table (https://www.ipcc-nggip.iges.or.jp/public/2019rf/vol4.html) and relevant literature (Bai et al., 2021; Eslamdoust & Sohrabi, 2018).

We aggregated carbon sequestration in soil organic carbon and biomass carbon across 4 SSPs to derive combined total carbon sequestration (megagrams per hectare). The results were further aggregated to a resolution of 1 km to align with the biodiversity data.

Recognizing biodiversity, carbon, and climate hotspots

A random sample of 2000 points in China-ASEAN was analyzed to examine the relationships among climate change vulnerability, species distribution potential, and carbon stock capacity. Scatter plots with LOESS regression trend lines and 95% confidence intervals were employed. Based on the species distribution potential, ecosystem vulnerability to climate change, and carbon stock capacity for each cell, we ranked the scores for each factor and selected the 30% of cells with the highest scores for biodiversity, carbon, and climate change vulnerability as hotspots in China-ASEAN. We chose 30% as the conservation target threshold because it ensures consistency in identifying hotspots for each conservation feature; aligns with the 30×30 target set by the KM-GBF, facilitating comparison of our 30×30 priority conservation areas and representativeness across different protection elements; and avoids the subjectivity and uncertainty associated with setting an experience-based threshold. We calculated pairwise Jaccard similarities for conservation priorities across the 4 SSP scenarios. Strong correlations represented spatially similar hotspot distributions, whereas weak correlations represented spatially divergent hotspot distributions.

Expansion scenarios and spatial prioritization

To assess the impact of spatial scale on the prioritization of areas for conservation, we considered regional, national, and biogeographical planning coordination scales. The regional scenario equally weighed regional biodiversity, carbon, and climate change vulnerability based on their value rankings across China-ASEAN. The national scenario allocated protection evenly across each country, ensuring that PAs were spread uniformly across the political landscape. The biogeographical scenario ensured even spatial representation from an ecological perspective by protecting equal portions of each biogeographical province.

We used a hierarchical mask layer to prioritize existing PAs before focusing on remaining cells. Data for the ASEAN region's PAs were sourced from the World Database on Protected Areas (WDPA; www.protectedplanet.net) (UNEP-WCMC & IUCN, 2024) and were supplemented by our database on China's PAs. Polygons of PAs were rasterized and projected onto a 1-km^2 grid. We concentrated our analyses on land in China-ASEAN that could accommodate future PAs. We excluded areas with high human disturbance. These areas were identified using the human footprint (HFP) index (Gassert et al., 2023), which considers, for example, land-cover change, population density, nighttime lights, roads, railways, and navigable rivers. The original 100-m resolution was upscaled up to 1 km. Cells with an HFP value >20, representing roughly 8.89% of the region, were excluded from our analyses (Eckert et al., 2023).

The remaining cells, representing largely intact ecosystems, were considered good candidates for protection. Because over 70% of Singapore's area has an HFP >20, the remaining area available for conservation planning was <30%. Thus, in the national scenario, we used an HFP threshold of 35 for Singapore, allowing 40% of the low-HFP area to be included in its conservation planning. We used the single-feature connectivity form and negexp kernel type for connectivity calculations in Zonation, and parameters were set to negexp (2, 10). Zonation 5 with additive benefit function ($z = 0.25$) marginal loss was employed to prioritize land in each conservation scenario (Kareksela et al., 2013; Moilanen et al., 2022). For national and biogeographical scenarios, subregions were used, where a full prioritization was performed for each subregion separately and then these prioritizations were combined into one final raster that represented all of China-ASEAN.

Data for administrative areas were obtained from Global Administrative Areas, and biogeographical boundaries were sourced from Udvardy's biogeographical provinces (Udvardy, 1975). These data were prepared by IUCN as a contribution to the UNESCO MAB Programme aimed at devising a satisfactory classification of the world's biotic areas for conservation purposes. The output of Zonation 5 is a raster of all unmasked cells ranked according to their priority. From these rank maps, we simulated the 30×30 scenario by selecting the 30% of cells with the highest conservation priority in each scenario, including already PAs. Although all rank maps were generated (available on request), we included only the 3 scales of planning scenarios under SSP245, based on the assumption that current socioeconomic development trends and emission reduction efforts will remain largely unchanged, resulting in a medium-emission scenario (projected global warming 2.5–3°C).

Conservation gaps in spatial commitments

To highlight the uneven challenges posed by changing conservation planning scales, we calculated the conservation gap for each country and the mean HFP per unprotected priority cell, mean population per unprotected priority cell, and area of the country's unprotected priority conservation areas divided by its per capita gross domestic product (GDP) under 3 spatial coordination scenarios.

RESULTS

Prediction of climate change vulnerability, species distribution, and carbon stock for 2030

Results for the intermediate SSP245 scenario showed a spatial pattern of climate change vulnerability for 2030 under the SSP245 scenario (Appendix S4). High climate change exposure values in China-ASEAN occurred primarily in the North China Plain, the Northeast China Plain, and the lowland areas of southern Indochina. High sensitivity values concentrated in urban areas. Adaptation values were significantly higher (Appendix S4) in high-elevation regions, such as the Yunnan–Guizhou Plateau, the southeastern hills of China, and the northern Indo-China Peninsula. Results for the intermediate SSP245 scenario showed a high species distribution potential across China-ASEAN, particularly in lowland areas and southern regions (Appendix S5). The distribution potential patterns for amphibians, birds, mammals, and reptiles were generally consistent at the regional scale. Values in tropical and subtropical climate zones were higher than in temperate and montane climate zones. Results for the intermediate SSP245 scenario showed a spatial pattern of carbon stock capacity from biomass carbon and soil carbon across China-ASEAN (Appendix S6). Soil carbon in China-ASEAN was primarily distributed in the lowland areas of Indonesia and the Great and Lesser Khingan Mountains in northeastern China. In contrast, biomass carbon was mainly found in the tropical rainforest climate zones and high-elevation areas of the Indo-China Peninsula.

Climate change vulnerability decreased as elevation increased and remained relatively the same across different latitudes; it was notably lower between longitudes 75° E and 100° E. Species distribution potential decreased as elevation increased but showed relatively large increases from 4000 to 5000 m elevation. It was highest between latitudes 11° S and 20° N, dropped at 20° N, and increased again between latitudes 40° N and 50° N. Species distribution potential was relatively high between longitudes 92° E and 122° E. Many areas with high species distribution potential overlapped with regions of high climate change vulnerability and coastal zones, making them susceptible to sea-level rise. These regions also faced intensive human activities and deforestation, rendering their habitats highly vulnerable to human impact. Carbon stock capacity was relatively similar across different elevation gradients, peaking between latitudes 11° S and 10° N and longitudes 93° E and 140° E.

Overlap in hotspots sites across conservation features

Correlation of climate change vulnerability, species distribution, and carbon stock capacity in China-ASEAN region under the SSP245 scenario showed that regions with high species distribution potential or carbon stock capacity tended to exhibit relatively higher climate change vulnerability (Appendix S7). Under SSP245, 56.31% of the land in China-ASEAN was in at least one of the climate, carbon, or species hotspots (Figure 2). Among these, cells where all 3 types of hotspots overlapped account for 6.59% of the region, primarily located in Indonesia, Malaysia, and Cambodia. Cells belonging to 2 types of hotspots constituted 20.73%. The highest amount of overlap was between species and carbon hotspots, followed by climate and species hotspots, and climate and carbon hotspots. The remaining 28.98% of cells belonged to only one type of hotspot, mainly distributed in China, Thailand, and Myanmar.

Variation in spatial priorities across scenarios

Areas with excessively high human footprints (8.40% of China-ASEAN), primarily located in Singapore and central and eastern China, were excluded (Appendix S8). The distribution of priority conservation areas under the SSP245 scenario exhibited different patterns across regional, national, and biogeographical scales (Figure 3). The priority rank maps across all coordinating scales and SSP scenarios are in Figshare (https://figshare.com/s/8fd20f32b3eb73b089f6). At the regional scale, newly identified priority lands were mainly distributed between 10° S and 10° N, where species and carbon hotspots were concentrated. Their distribution was minimal in China and Indochina. At the national scale, newly identified priority lands peaked between 20° N and 30° N, primarily because, under the national scenario, China, the largest country in the region, had its newly identified priority lands mainly distributed in the southeastern hills. Although this area is not a hotspot for species and carbon in the region, it is undoubtedly one of the most valuable areas for conservation in China. At the biogeographical scale, newly identified priority lands were relatively uniformly distributed across latitudes and longitudes.

The distribution of 30×30 priority land was predominantly concentrated at lower elevations across all SSP scenarios and spatial scales (Appendix S9a–c), with a marked decrease in priority land area as elevation increased. The peak around 5000 m was primarily due to a significant portion of China's existing PAs being located on the Qinghai–Tibet Plateau, where elevations are high. The correlations of the priority land spatial distribution for each SSP scenario under the 3 coordinating scales showed that the distribution of priority land was highly correlated across the 4 SSP scenarios. The highest correlation occurred at the regional scale, followed by the national scale and biogeographical scale (Appendix S9d–f). In contrast, the influence of different SSP scenarios on these priorities was minimal.
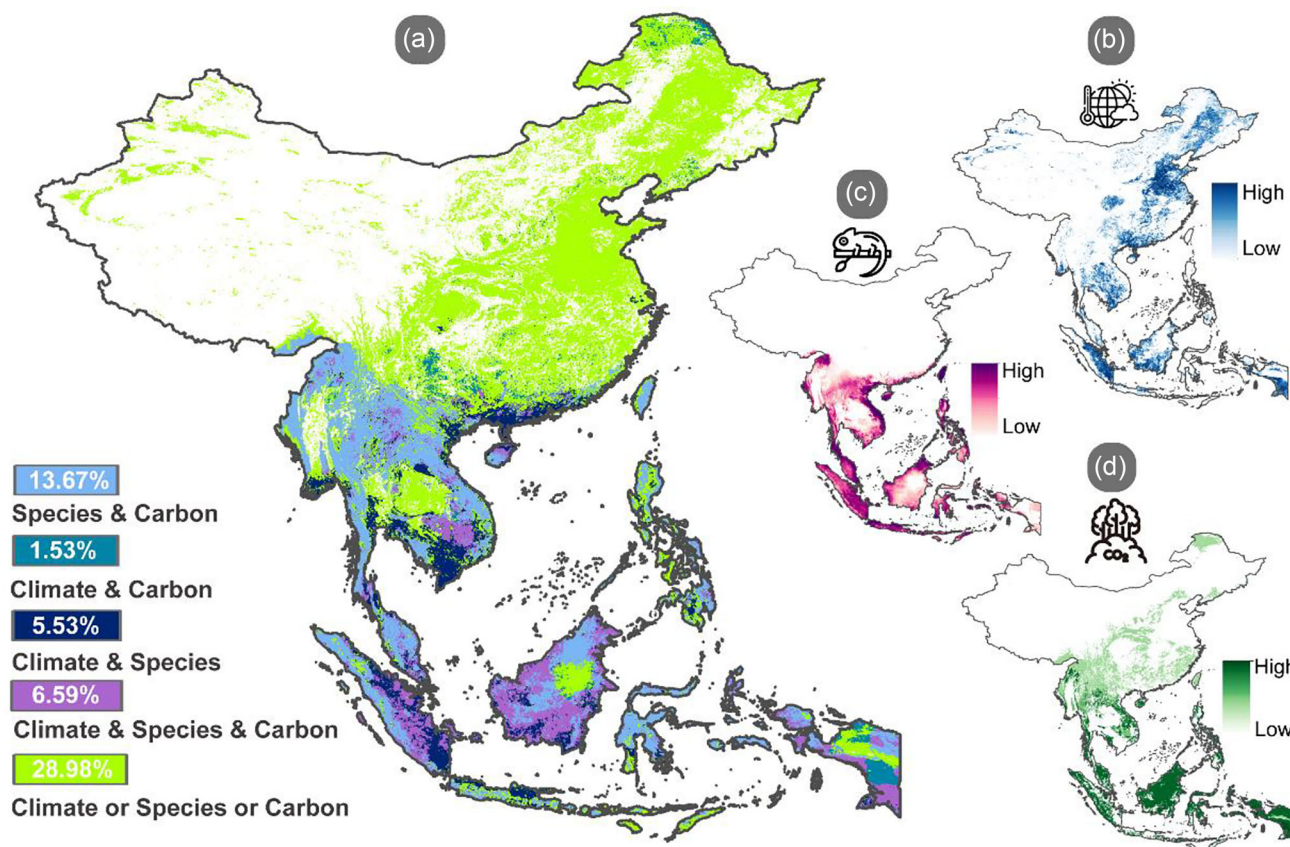
FIGURE 2 In China and the Association of Southeast Asian Nations (China-ASEAN), (a) overlay of climate change vulnerability, species distribution potential, and carbon stock capacity hotspots, (b) distribution of climate change vulnerability hotspots and their value rank, (c) distribution of species distribution potential hotspots and their value rank, and (d) distribution of carbon stock capacity hotspots and their value ranking. Climate, biodiversity, and carbon hotspots were identified, respectively, by selecting the 30% of areas with the highest climate change vulnerability, species distribution potential, and carbon stock capacity.

Regardless of SSP, the conservation priorities identified by our framework remained relatively stable.

Limited existing protection and large conservation gains under 30×30

The existing PAs, covering 15.49% of China-ASEAN's terrestrial land, contained 12.45% of the 2030 species hotspots and 14.56% of the 2030 carbon hotspots. Representation of climate hotspots was lower, at just 7.00% (Figure 4). Thus, there was some conservation of carbon storage but a significant shortfall in biodiversity conservation and a clear deficiency in addressing climate change and protecting vulnerable areas. Under regional planning, species hotspot protection increased by 20.70–33.15% (Figure 4b). At the national scale, protected carbon hotspots increased by 20.85–35.41% (Figure 4c). The increase in protection percentage for climate hotspots was around 15.00% across all 3 planning scales, with little difference among them. Although biogeographical scale planning did not provide the largest increase in representation for any of the conservation hotspots relative to the regional and national scales, it ensured the protection of 30% of each biogeographical province, thereby increasing the ecosystem and biota representativeness of the PA network. In contrast, at the regional scale, 16 out of 25 (64%) biogeographical provinces in China-ASEAN had PA coverage below 30%. Similarly, at the national scale, 12 out of 25 (48%) biogeographical provinces had PA coverage below 30%.

Appraisal of administration-level conservation gaps

Identifying priorities at different planning scales resulted in significant variations in administration-level conservation gaps. At the regional coordinating scale (Figure 5a), Singapore and China almost would not need to increase their PAs to meet the 30×30 target, whereas Cambodia, the Philippines, Laos, Indonesia, Brunei, and Malaysia would need to increase their national areas by 14.32–65.59% to achieve 30% protection of their land. Particularly in Cambodia, where existing PAs already cover 39.62% of the country's land (the only country among the 12 in China-ASEAN to have reached the 30% target), further increases in PA would still be required under regional-scale planning.
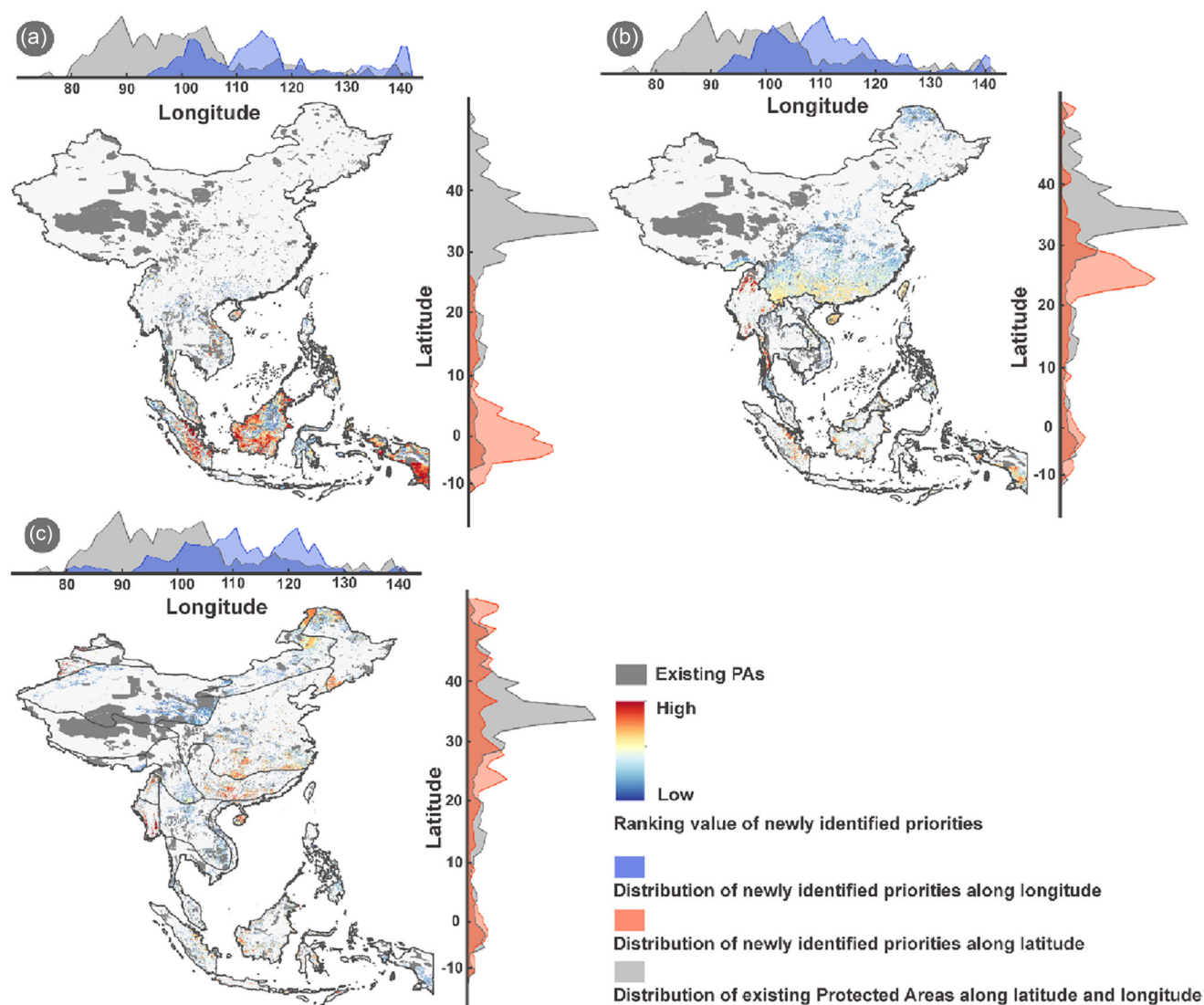
FIGURE 3   In China and the Association of Southeast Asian Nations (China-ASEAN), spatial priorities for (a) regional protection coordination, (b) national protection coordination, and (c) biogeographical protection coordination and their latitude and longitude (dark gray, existing PAs in the conservation priority areas; blue to red shading, rank of newly identified areas of conservation priority; coordinate axis gray, distribution of existing protected areas; coordinate axis red, distribution of newly identified priorities; coordinate axis blue, distribution of newly identified priorities).

To achieve the 30×30 priorities under the national planning scale (Figure 5b), each country would need to ensure that PAs covered 30% of its own land area, resulting in conservation gaps ranging from 0% to 24.48%. Vietnam, Malaysia, Indonesia, Myanmar, and Singapore currently have protection proportions below 15%, requiring increases of 15.11%, 17.18%, 18.24%, 23.39%, and 24.48%, respectively, to fill the conservation gaps under the national planning scale. Under the biogeographical coordinating scale (Figure 5c), the average gap across countries was 13.14%, smaller than the 23.29% under the regional scale and 14.25% under the national scale. Thailand, Vietnam, and Singapore had the smallest conservation gaps, at 4.14%, 6.81%, and 7.52%, respectively. Laos, Timor-Leste, and Malaysia had the largest conservation gaps, at 21.55%, 18.40%, and 17.39%, respectively.

Practical considerations for on-the-ground implementation

At the national coordinating scale, the average HFP value per newly identified conservation priority cell varied greatly across countries (Figure 6a), ranging from 2.63 in Brunei to a maximum of 50 in Singapore. At the biogeographical planning scale, the HFP value per newly identified priority cell for each country was below 13%. The countries with the highest HFP value per newly identified priority cell at regional, national, and biogeographical planning scales were Malaysia, Singapore, and Timor-Leste, respectively.

Regarding the average human population per newly identified priority cell (Figure 6b), Indonesia had the highest at the regional scale (10.45/km^2), and Singapore had the highest at the
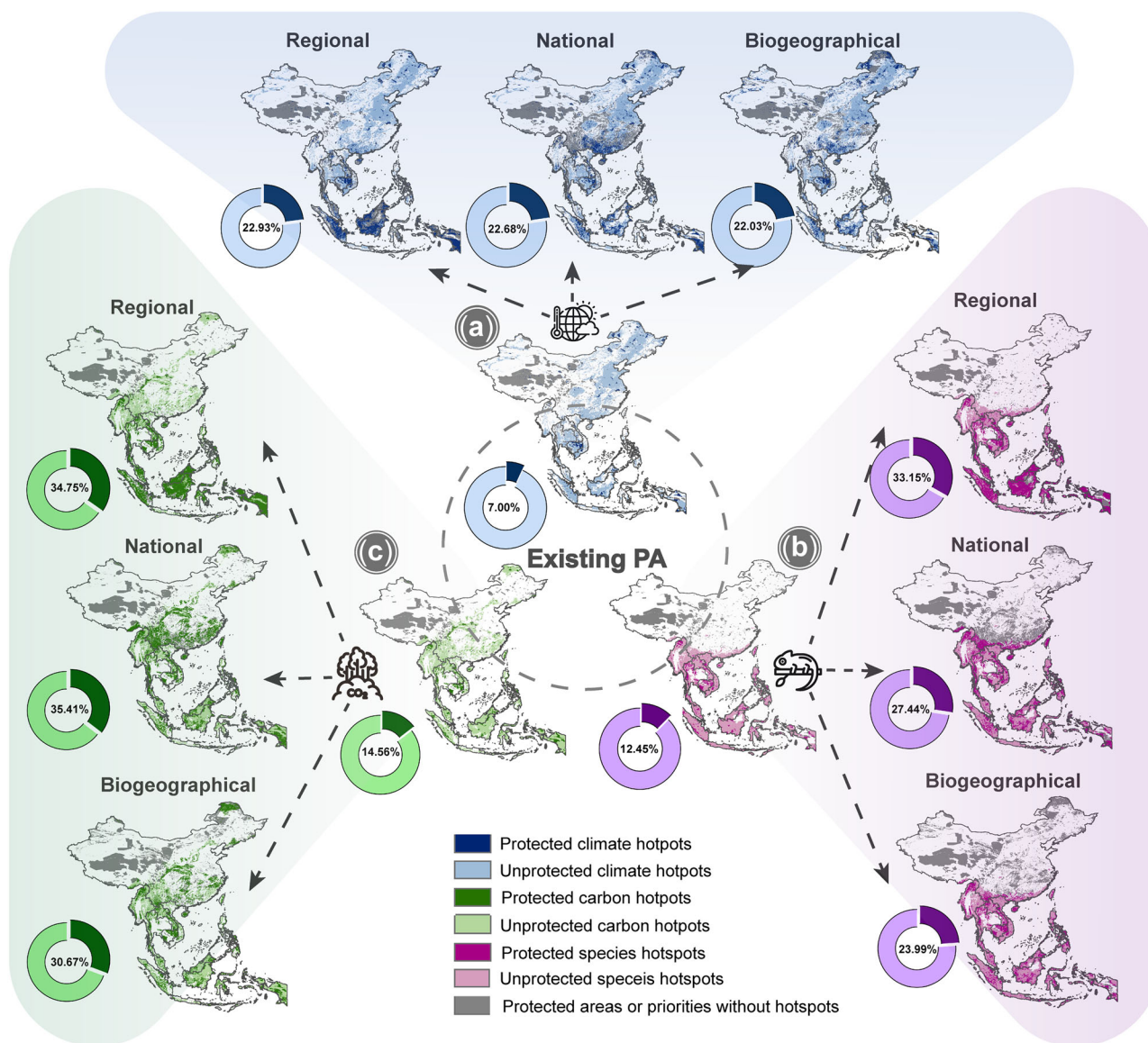
FIGURE 4 For China and the Association of Southeast Asian Nations (China-ASEAN) and under the SSP245 (Shared Socioeconomic Pathway) scenario, (a) hotspots of climate change vulnerability (climate hotspots), (b) hotspots of species distribution potential (species hotspots), and (c) hotspots of carbon stock capacity (carbon hotspots) in existing PAs and regional, national, and biogeographical priority conservation area (percentages in donut charts, percentages of climate [blue], species [purple], and carbon [green] hotspots in protected [dark shade] and unprotected [light shade] areas).

national and biogeographical scales (exceeding $1000/km^2$). In contrast, other countries had an average population density per newly identified priority cell below 10 people/km^2 at all spatial scales. At the regional scale, the top 3 countries with the highest area of the country's unprotected priority areas divided by their per capita GDP (Figure 6c) were Indonesia, Myanmar, and Laos. At the national and biogeographical scales, the 3 with the most such areas were Myanmar, China, and Indonesia. Due to its small land area and high per capita GDP, Singapore had the smallest mean newly identified priority area per capita GDP across all 3 spatial scales.

DISCUSSION

Integrating climate adaptation in KM-GBF implementation

Although there is strong evidence that PAs have protected biodiversity from land-use disturbances (Watson et al., 2014), they remain vulnerable to future climate change. Over 50% of terrestrial PAs globally are unlikely to adequately conserve biodiversity in the face of future climate change (Parks et al., 2023). Our framework's priority patterns exhibited significant spatial
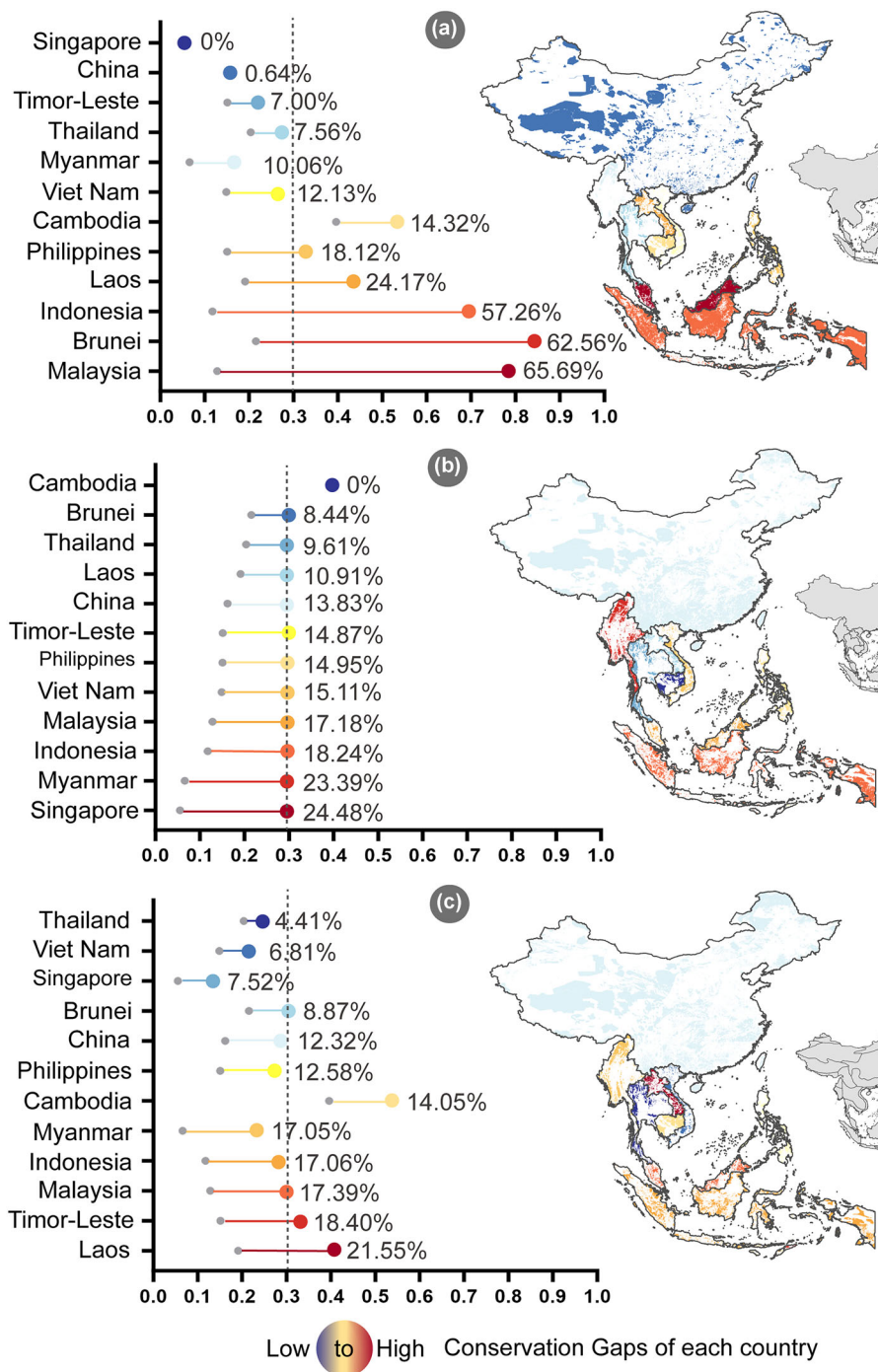
FIGURE 5 In China and the Association of Southeast Asian Nations (China-ASEAN) for the 30×30 target under the SSP245 (Shared Socioeconomic Pathway) scenario: (a) regional, (b) national, and (c) biogeographical gaps in conservation area (gray dots, current protection proportion for each country; blue to red shading, proportion a country needs to protect to achieve the 30×30 target at each scale; length of colored lines to gray dots, relative size of conservation gap; countries arranged from top to bottom according to increasing gap size; gray dashed line, 30% protection area target).

distribution differences compared with the results of studies (Voskamp et al., 2023; Zeng et al., 2022; Zhu et al., 2021) that did not incorporate future climate scenarios, underscoring the necessity of integrating climate projections in conservation planning. Our findings suggest that the 30×30 commitment could greatly enhance biodiversity conservation and promote

climate-smart spatial planning, but this depends on designing PA networks that address the vulnerability of biodiversity and ecosystems to future climate impacts (Hannah et al., 2007; Stralberg et al., 2020). Although activities like illegal logging and pollution can be managed with short-term legislation, climate change affects entire ecological networks and services, which
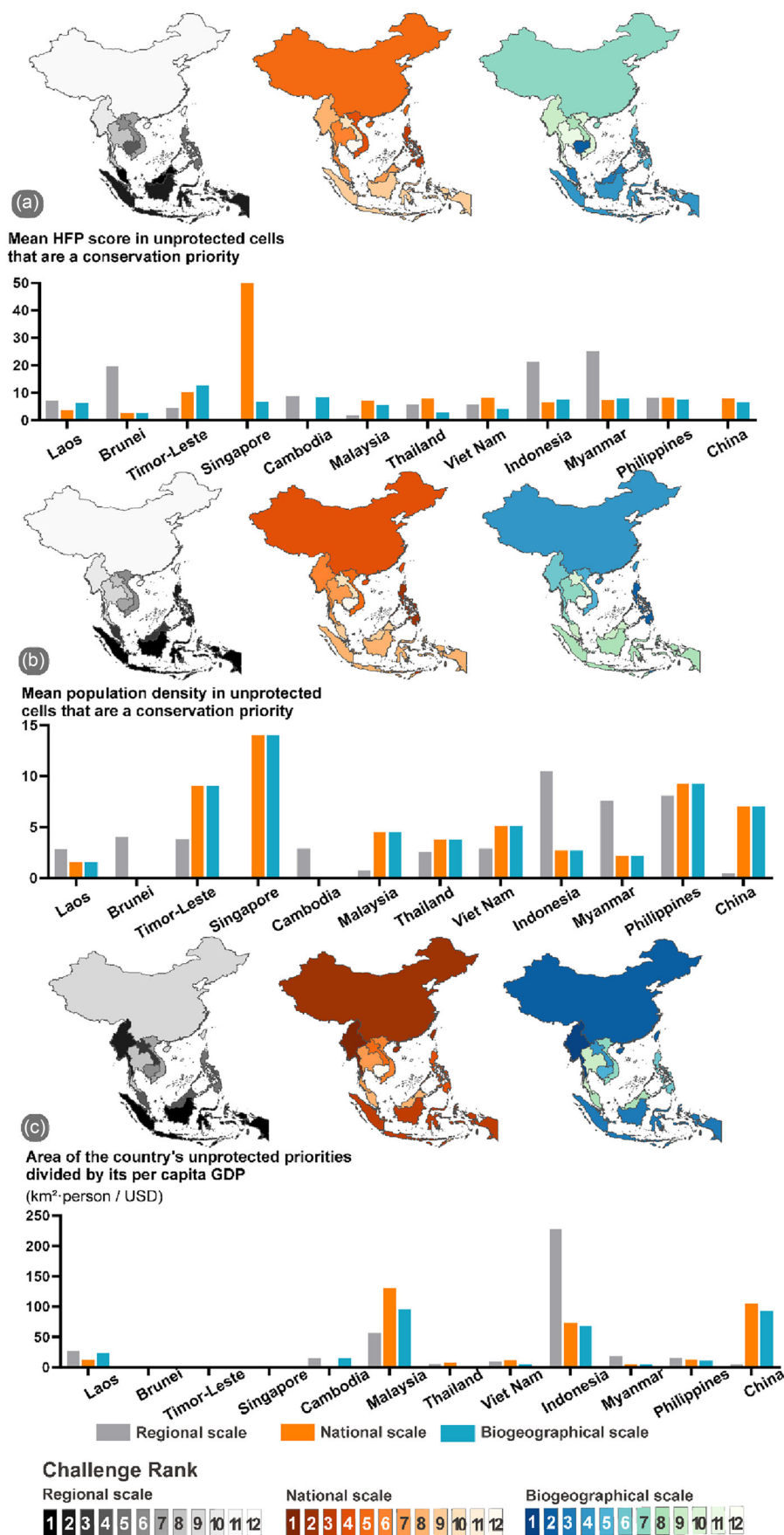
FIGURE 6 The challenges faced by countries in China and the Association of Southeast Asian Nations (China-ASEAN) in meeting the 30×30 target at different scales: (a) mean human footprint (HFP) score in unprotected cells that are a conservation priority, (b) mean population density in unprotected cells that are

(Continues)

FIGURE 6   (Continued)

a conservation priority, and (c) area of the country's unprotected priorities divided by its per capita GDP and the challenge ranks (maps) of these metrics (higher ranks indicate greater challenges in bridging conservation gaps) regionally (left), nationally (middle), and biographically (right).

demands flexible, long-term conservation planning (Rosales, 2008; Dobrowski et al., 2021).

Climate-adaptive conservation can generate spillover effects by enhancing the resilience of natural resources and ecosystem services, such as agriculture, fisheries, and tourism, which many communities in China-ASEAN rely on, thereby benefiting both local livelihoods and regional economies. The conservation priorities we identified exhibited relatively consistent spatial distribution across different SSP scenarios (Michalak et al., 2020). This contrasts with previous global and regional studies that identified future climate refugia and habitat, where the spatial patterns often changed significantly with different SSP scenario climate data. Our findings suggested that our integrated framework, which incorporates climate change vulnerability, species distribution, and carbon stock, is promising for designing robust conservation priority models that remain relatively insensitive to uncertainties in future climate models.

However, translating these insights into actionable policies under the KM-GBF presents significant challenges. The Draft Decision on the Monitoring Framework for the KM-GBF, presented at COP16 in November 2024, revealed limited integration of climate-change-related metrics and indicators across its goals and targets. For target 3 (the 30×30 commitment), existing indicators primarily emphasize static dimensions, such as the protected connected index, PA connectedness index, and species protection index, and there is minimal consideration of dynamic ecological processes influenced by climate change. This limitation extends to the entire framework, where most climate-related indicators, aside from the BERI (Ferrier et al., 2020), are qualitative, binary, and confined to national scales, which limits their utility in addressing dynamic climate impacts. By contrast, the indices we propose—integrating climate change exposure, sensitivity, and adaptation metrics—are scientifically robust, data accessible, and scalable. These dynamic metrics address critical gaps and hold significant potential for enhancing KM-GBF's indicators, paving the way for a more comprehensive and adaptive framework that effectively supports biodiversity conservation under changing climate conditions.

Importance of protection planning

Our results showed that the success of the 30×30 commitment and the achievement of the expected conservation outcomes will depend on how effectively countries coordinate conservation efforts and determine spatial priorities. Decisions on conservation objectives and the design of 30×30 schemes at different spatial scales significantly influenced the identification of areas of conservation priority, corroborating results of previous studies that highlight disparities in spatial priorities across scales (Eckert et al., 2023; Shen et al., 2023). National strategies were considerably more feasible compared with regional

coordination because planning within a country is far easier than planning among countries. For regions with vastly different economic, political, and sociocultural conditions, widespread comprehensive cross-border actions are unlikely (Mason et al., 2020). Our results suggest that a transnational coordinating approach based on biogeographical provinces could lead to high coverage of conservation feature hotspots and representation of ecosystem types. Unlike other transnational approaches, such as those at regional or global scales, our method does not assign excessively high or nearly unachievable conservation targets to countries with high biodiversity value, such as megadiverse countries. Conservation efforts often involve multiple conservation objectives and stakeholders, ranging from biodiversity protection and climate change tackling to rights of Indigenous people and economic development (Wang et al., 2024; Yang et al., 2020). In addressing such a complex ecological and socioeconomic challenge, it becomes evident that the choice of spatial extent of conservation planning is important (Carvalho et al., 2019).

Climate change is a global issue with impacts that transcend national borders, necessitating collaborative efforts that go beyond the capacity of individual countries. Regional protection coordination offers a pathway to achieve synergies across administrative and jurisdictional boundaries by connecting climate corridors and facilitating cross-border migration of species. For example, connectivity corridors, such as the Malaysia–Thailand transboundary corridor linking Taman Negara and Hala-Bala National Parks, or the China–Laos corridor connecting Xishuangbanna and northern Laos, provide practical examples of how transboundary conservation efforts can enhance connectivity between PAs. These corridors not only strengthen the resilience of individual PAs but also bolster the overall resilience of the conservation network by accommodating species migration and mitigating climate change impacts (Watson et al., 2021). China's initiative to establish the world's largest national park system by 2035 provides a model of how dynamic conservation strategies—such as connectivity corridors and climate-informed planning—can simultaneously support biodiversity conservation and climate resilience at scale. These approaches are equally applicable to the broader China-ASEAN region.

Need for an inclusive approach to 30×30

Although safeguarding global biodiversity is a global necessity, individual countries bear the responsibility of achieving 30×30 in their territories and must make rapid progress to do so in less than a decade (UNCBD., 2022). However, the sole focus on increasing PA coverage as a conservation objective is increasingly being met with resistance from Indigenous peoples and related organizations. By assessing the area of unprotected pri-

orities in relation to national per capita GDP levels, as well as the average HFP and population density of unprotected priority areas, our research highlights the possible challenges countries may face in achieving the conservation targets outlined in the KM-GBF across various coordinating scales. Exploration of diversified conservation mechanisms, such as China's Ecological Conservation Redline (ECRL), which implements varying levels of conservation measures tailored to specific conservation priorities to ensure no change in land cover, offers valuable insights and reference cases for other regions facing similar challenges (Gao, 2019). China's ECRL project, proposed by scientists in 2000 and approved by the State Council in 2011, covers approximately 30% of China's land area now. Its management objectives include maintaining land-cover status quo, preventing net loss of biodiversity, and avoiding degradation of other ecosystem services within the ECRL. The management approaches under ECRL vary, encompassing strictly protected, minimally disturbed areas, as well as watershed protection zones permitting some agricultural and limited other human activities. Faced with conflicts between conservation and development in the implementation of ECRL, China is exploring large-scale market-based mechanisms for ecological compensation payments.

Limitations

We presented a multiscale framework for bridging conservation gaps under the 30×30 commitment in China-ASEAN and addressing the dynamic challenges posed by climate change. By highlighting the importance of integrating climate adaptation metrics in spatial planning, we demonstrated how coordinated efforts at regional, national, and biogeographical scales can enhance PA networks' resilience and representativeness. Our framework not only provides a pathway to achieve equitable and effective 30×30 targets but also offers valuable insights for broader conservation strategies under the KM-GBF.

Although we focused on China-ASEAN, our workflow theoretically can be applied to any country to promote 30×30 planning. However, effective spatial planning relies on modeling for various conservation objectives. It must be acknowledged that significant data biases may still exist. For instance, we did not assess the extent of extrapolation in species distribution modeling with MaxEnt's MESS tool (Elith et al., 2010), which we will do in future work to improve projection accuracy. Although we provided a regional-scale assessment of climate change vulnerability, our focus was on nonspecies-specific regional vulnerability to climate change, rather than species-level or ecosystem vulnerability, in terms of biotic elements (Nicholson et al., 2021). Although we covered multiple conservation features highlighted in the KM-GBF, including biodiversity, ecosystem services, climate change, human impacts, and connectivity, we did not consider multiple dimensions of biodiversity, such as taxonomic diversity, functional diversity, and phylogenetic diversity (Jetz et al., 2022). More work is required to determine how multidimensional biodiversity priorities contrast with other 30×30 priorities. Additionally,

biodiversity in PAs may be affected by human activities in- and outside PAs, whether nearby or far away. The integrated framework of metacoupling can help address such challenges and improve the design of the 30×30 priorities (Liu, 2023).

ORCID

Hui Wu https://orcid.org/0000-0001-7591-3398
Xiaoli Shen https://orcid.org/0000-0003-2749-1121
Jianqiao Zhao https://orcid.org/0000-0002-5790-7880
Keping Ma https://orcid.org/0000-0001-9112-5340

REFERENCES

Allan, J. R., Possingham, H. P., Atkinson, S. C., Waldron, A., Di Marco, M., Butchart, S. H. M., Adams, V. M., & Kissling, W. D. (2022). The minimum land area requiring conservation attention to safeguard biodiversity. *Science*, *376*, 1094–1101.

Bai, Y., Fang, Z., & Hughes, A. C. (2021). Ecological redlines provide a mechanism to maximize conservation gains in Mainland Southeast Asia. *One Earth*, *4*(10), 1491–1504.

Baynham-Herd, Z., Amano, T., Sutherland, W. J., & Donald, P. F. (2018). Governance explains variation in national responses to the biodiversity crisis. *Environmental Conservation*, *45*(4), 307–314.

Bowler, D. E., Hof, C., Haase, P., Kröncke, I., Schweiger, O., Adrian, R., Baert, L., Bauer, H. G., Blick, T., Brooker, R. W., Dekoninck, W., Domisch, S., Eckmann, R., Hendrickx, F., Hickler, T., Klotz, S., Kraberg, A., Kühn, I., Matesanz, S., … Böhning-Gaese, K. (2017). Cross-realm assessment of climate change impacts on species' abundance trends. *Nature Ecology and Evolution*, *1*(3), Article 0067.

Brito-Morales, I., García Molinos, J., Schoeman, D. S., Burrows, M. T., Poloczanska, E. S., Brown, C. J., Ferrier, S., Harwood, T. D., Klein, C. J., McDonald-Madden, E., Moore, P. J., Pandolfi, J. M., Watson, J. E. M., Wenger, A. S., & Richardson, A. J. (2018). Climate velocity can inform conservation in a warming world. *Trends in Ecology & Evolution*, *33*, 441–457.

Burrows, M. T., Schoeman, D. S., Buckley, L. B., Moore, P., Poloczanska, E. S., Brander, K. M., Brown, C., Bruno, J. F., Duarte, C. M., Halpern, B. S., Holding, J., Kappel, C. V., Kiessling, W., O'Connor, M. I., Pandolfi, J. M., Parmesan, C., Schwing, F. B., Sydeman, W. J., & Richardson, A. J. (2011). The pace of shifting climate in marine and terrestrial ecosystems. *Science*, *334*, 652–656.

Carrasco, L., Papeş, M., Sheldon, K. S., & Giam, X. (2021). Global progress in incorporating climate adaptation into land protection for biodiversity since Aichi targets. *Global Change Biology*, *27*(9), 1788–1801.

Carroll, C., Roberts, D. R., Michalak, J. L., Lawler, J. J., Nielsen, S. E., Stralberg, D., Hamann, A., Mcrae, B. H., & Wang, T. (2017). Scale-dependent complementarity of climatic velocity and environmental diversity for identifying priority areas for conservation under climate change. *Global Change Biology*, *23*(11), 4508–4520.

Carvalho, J. S., Graham, B., Rebelo, H., Bocksberger, G., Meyer, C. F. J., Wich, S., & Kühl, H. S. (2019). A global risk assessment of primates under climate and land use/cover scenarios. *Global Change Biology*, *25*(9), 3163–3178.

Chen, G., Li, X., & Liu, X. (2022). Global land projection based on plant functional types with a 1-km resolution under socio-climatic scenarios. *Scientific Data*, *9*(1), Article 125.

Convertino, M., Muñoz-Carpena, R., Chu-Agor, M. L., Kiker, G. A., & Linkov, I. (2014). Untangling drivers of species distributions: Global sensitivity and uncertainty analyses of maxent. *Environmental Modelling & Software*, *51*(1), 296–309.

D'Agata, S., & Maina, J. M. (2022). Climate change reduces the conservation benefits of tropical coastal ecosystems. *One Earth*, *5*(11), 1228–1238.

Dobrowski, S. Z., Littlefield, C. E., Lyons, D. S., Hollenberg, C., Carroll, C., Parks, S. A., Abatzoglou, J. T., Hegewisch, K., & Gage, J. (2021). Protected-area targets could be undermined by climate change-driven shifts in ecoregions and biomes. *Communications Earth & Environment*, *2*, Article 198.

Doughty, C. E. (2015). Drought impact on forest carbon dynamics and fluxes in Amazonia. *Nature*, *519*, 78–82.

Eckert, I., Pollock, L. J., Brown, A., Caron, D., & Riva, F. (2023). 30×30 biodiversity gains rely on national coordination. *Nature Communications*, *14*, Article 7113.

Elith, J., Kearney, M., & Phillips, S. (2010). The art of modelling range-shifting species. *Methods in Ecology and Evolution*, *1*, 330–342.

Elsen, P. R., Farwell, L. S., Pidgeon, A. M., & Radeloff, V. C. (2021). Contrasting seasonal patterns of relative temperature and thermal heterogeneity and their influence on breeding and winter bird richness patterns across the conterminous United States. *Ecography*, *44*(6), 953–965.

Elsen, P. R., Monahan, W. B., Dougherty, E. R., & Merenlender, A. M. (2020). Keeping pace with climate change in global terrestrial protected areas. *Science Advances*, *6*(25), Article eaay0814.

Eslamdoust, J., & Sohrabi, H. (2018). Carbon storage in biomass, litter, and soil of different native and introduced fast-growing tree plantations in the South Caspian Sea. *Journal of Forestry Research*, *29*, 449–457.

Farhadinia, M. S., Maheshwari, A., Nawaz, M. A., Ambarlı, H., Gritsina, M. A., Koshkin, M. A., Rosen, T., Hinsley, A., & Macdonald, D. W. (2019). Belt and Road Initiative may create new supplies for illegal wildlife trade in large carnivores. *Nature Ecology & Evolution*, *3*(9), 1267–1268.

Feng, Y., Ziegler, A. D., Elsen, P. R., Liu, Y., He, X., Spracklen, D. V., Holden, J., Jiang, X., Zheng, C., & Zeng, Z. (2021). Upward expansion and acceleration of forest clearance in the mountains of Southeast Asia. *Nature Sustainability*, *4*, 892–899.

Ferrier, S., Harwood, T. D., Ware, C., & Hoskins, A. J. (2020). A globally applicable indicator of the capacity of terrestrial ecosystems to retain biological diversity under climate change: The bioclimatic ecosystem resilience index. *Ecological Indicators*, *117*(2020), Article 106554.

Gao, J. (2019). How China will protect one-quarter of its land. *Nature*, *569*, Article 457.

Gao, J., Zuo, L., & Liu, W. (2021). Environmental determinants impacting the spatial heterogeneity of karst ecosystem services in Southwest China. *Land Degradation and Development*, *32*(4), 1718–1731.

Gassert, F., Venter, O., Watson, J. E. M., Brumby, S. P., Mazzariello, J. C., Atkinson, S. C., & Hyde, S. (2023). An operational approach to near real time global high resolution mapping of the terrestrial Human Footprint. *Frontiers in Remote Sensing*, *4*, Article 1130896.

Hannah, L., Midgley, G., Andelman, S., Araújo, M., Hughes, G., Martinez-Meyer, E., Pearson, R., & Williams, P. (2007). Protected area needs in a changing climate. *Frontiers in Ecology and the Environment*, *5*(3), 131–138.

Hengl, T., & Nauman, T. (2019). *Predicted USDA soil orders at 250 m (probabilities) (version v0.1)*. Zenodo. https://doi.org/10.5281/zenodo.2658183

Hengl, T., & Wheeler, I. (2018). *Soil organic carbon stock in kg/m2 for 5 standard depth intervals (0–10, 10–30, 30–60, 60–100 and 100–200 cm) at 250 m resolution*. Zenodo. https://doi.org/10.5281/zenodo.2536040

Hudson, L. N., Newbold, T., Contu, S., Hill, S. L. L., Lysenko, I., De Palma, A., Phillips, H. R. P., Senior, R. A., Bennett, D. J., Booth, H., Choimes, A., Correia, D. L. P., Day, J., Echeverría-Londoño, S., Garon, M., Harrison, M. L. K., Ingram, D. J., Jung, M., Kemp, V., … Purvis, A. (2017). The database of the PREDICTS (Projecting Responses of Ecological Diversity In Changing Terrestrial Systems) project. *Ecology and Evolution*, *7*(1), 145–188.

Ippolito, A., Sala, S., Faber, J. H., & Vighi, M. (2010). Ecological vulnerability analysis: A river basin case study. *Science of the Total Environment*, *408*, 3880–3890.

Jetz, W., McGowan, J., Rinnan, D. S., Possingham, H. P., Visconti, P., O'Donnell, B., & Londoño-Murcia, M. C. (2022). Include biodiversity representation indicators in area-based conservation targets. *Nature Ecology & Evolution*, *6*, 123–126.

Jones, C., Lowe, J., Liddicoat, S., & Betts, R. (2009). Committed terrestrial ecosystem changes due to climate change. *Nature Geoscience*, *2*(7), 484–487.

Jung, M., Arnell, A., Lamo, X. D., García-rangel, S., Lewis, M., Mark, J., Merow, C., Miles, L., Ondo, I., Pironon, S., Ravilious, C., Rivers, M., Schepaschenko, D., Tallowin, O., Soesbergen, A. V., Govaerts, R., Boyle, B. L., Enquist, B. J., Feng, X., … Visconti, P. (2021). Areas of global importance for conserving terrestrial biodiversity, carbon and water. *Nature Ecology & Evolution*, *5*(11), 1499–1509.

Kareksela, S., Moilanen, A., Tuominen, S., & Kotiaho, J. S. (2013). Use of Inverse spatial conservation prioritization to avoid biodiversity loss outside protected areas. *Conservation Biology*, *27*, 1294–1303.

Keppel, G., Van Niel, K. P., Wardell-Johnson, G. W., Yates, C. J., Byrne, M., Mucina, L., Schut, A. G. T., Hopper, S. D., & Franklin, S. E. (2011). Refugia: Identifying and understanding safe havens for biodiversity under climate change. *Global Ecology and Biogeography*, *21*, 393–404.

Li, D., Wu, S., Liu, L., Zhang, Y., & Li, S. (2018). Vulnerability of the global terrestrial ecosystems to climate change. *Global Change Biology*, *24*(9), 4095–4106.

Liu, J. (2023). Leveraging the metacoupling framework for sustainability science and global sustainable development. *National Science Review*, *10*, Article nwad090.

Loarie, S. R., Duffy, P. B., Hamilton, H., Asner, G. P., Field, C. B., & Ackerly, D. D. (2009). The velocity of climate change. *Nature*, *462*(7276), 1052–1055.

MacKey, B., Berry, S., Hugh, S., Ferrier, S., Harwood, T. D., & Williams, K. J. (2012). Ecosystem greenspots: Identifying potential drought, fire, and climate-change micro-refuges. *Ecological Applications*, *22*(6), 1852–1864.

Mason, N., Ward, M., Watson, J. E. M., Venter, O., & Runting, R. K. (2020). Global opportunities and challenges for transboundary conservation. *Nature Ecology & Evolution*, *4*(5), 694–701.

Menzel, A., Sparks, T. H., Estrella, N., & Roy, D. B. (2006). Altered geographic and temporal variability in phenology in response to climate change. *Global Ecology and Biogeography*, *15*, 498–504.

Michalak, J. L., Stralberg, D., Cartwright, J. M., & Lawler, J. J. (2020). Combining physical and species-based approaches improves refugia identification. *Frontiers in Ecology and the Environment*, *18*, 254–260.

Moilanen, A., Lehtinen, P., Kohonen, I., Jalkanen, J., Virtanen, E. A., & Kujala, H. (2022). Novel methods for spatial prioritization with applications in conservation, land use planning and ecological impact avoidance. *Methods in Ecology and Evolution*, *13*(5), 1062–1072.

Mulligan, M. (2013). WaterWorld: A self-parameterising, physically based model for application in data-poor but problem-rich environments globally. *Hydrology Research*, *44*, 748–769.

Naidoo, R., Gerkey, D., Hole, D., Pfaff, A., Ellis, A. M., Golden, C. D., Herrera, D., Johnson, K., Mulligan, M., Ricketts, T. H., & Fisher, B. (2019). Evaluating the impacts of protected areas on human well-being across the developing world. *Science Advances*, *5*(4), Article eaav3006.

Natural Capital Project. (2024). *InVEST 0.0*. Stanford University, University of Minnesota, Chinese Academy of Sciences, The Nature Conservancy, World Wildlife Fund, Stockholm Resilience Centre and the Royal Swedish Academy of Sciences. https://naturalcapitalproject.stanford.edu/software/invest

Nicholson, E., Watermeyer, K. E., Rowland, J. A., Sato, C. F., Stevenson, S. L., Andrade, A., Brooks, T. M., Burgess, N. D., Cheng, S. T., Grantham, H. S., Hill, S. L., Keith, D. A., Maron, M., Metzke, D., Murray, N. J., Nelson, C. R., Obura, D., Plumptre, A., Skowno, A. L., & Watson, J. E. M. (2021). Scientific foundations for an ecosystem goal, milestones and indicators for the post-2020 global biodiversity framework. *Nature Ecology and Evolution*, *5*(10), 1338–1349.

Parks, S. A., Holsinger, L. M., Abatzoglou, J. T., Littlefield, C. E., & Zeller, K. A. (2023). Protected areas not likely to serve as steppingstones for species undergoing climate-induced range shifts. *Global Change Biology*, *29*, 2681–2696.

Phillips, S. J., Anderson, R. P., Dudík, M., Schapire, R. E., & Blair, M. E. (2017). Opening the black box: An open-source release of Maxent. *Ecography*, *40*, 887–893.

Phillips, S. J., Anderson, R. P., & Schapire, R. E. (2006). Maximum entropy modeling of species geographic distributions. *Ecological Modelling*, *190*, 231–259.

Reed, T. E., Grøtan, V., Jenouvrier, S., Sæther, B.-E., & Visser, M. E. (2013). Population growth in a wild bird is buffered against phenological mismatch. *Science*, *340*, 488–491.

Rosales, J. (2008). Economic growth, climate change, biodiversity loss: Distributive justice for the global north and south. *Conservation Biology*, *22*(6), 1409–1417.

Sahr, K. (2018). *DGGRID*. Southern Terra Cognita Laboratory. www.discreteglobalgrids.org

Sandel, B. (2011). The influence of late quaternary climate-change velocity on species endemism. *Science*, *334*, 660–664.

Sasmito, S. D., Basyuni, M., Kridalaksana, A., Saragi-Sasmito, M. F., Lovelock, C. E., & Murdiyarso, D. (2023). Challenges and opportunities for achieving Sustainable Development Goals through restoration of Indonesia's mangroves. *Nature Ecology & Evolution*, *7*, 62–70.

Shen, X., Liu, M., Hanson, J. O., Wang, J., Locke, H., Watson, J. E. M., Ellis, E. C., Li, S., & Ma, K. (2023). Countries' differentiated responsibilities to fulfill area-based conservation targets of the Kunming-Montreal Global Biodiversity Framework. *One Earth*, *6*(5), 548–559.

Stralberg, D., Carroll, C., & Nielsen, S. E. (2020). Toward a climate-informed North American protected areas network: Incorporating climate-change refugia and corridors in conservation planning. *Conservation Letters*, *13*, Article e12712.

Thackeray, S. J., Sparks, T. H., Frederiksen, M., Burthe, S., Bacon, P. J., Bell, J. R., Botham, M. S., Brereton, T. M., Bright, P. W., Carvalho, L., Clutton-Brock, T., Dawson, A., Edwards, M., Elliott, J. M., Harrington, R., Johns, D., Jones, I. D., Jones, J. T., Leech, D. I., … Wanless, S. (2010). Trophic level asynchrony in rates of phenological change for marine, freshwater and terrestrial environments. *Global Change Biology*, *16*, 3304–3313.

Udvardy, M. D. F. (1975). *A classification of the biogeographical provinces of the world* (Occasional Paper 18). International Union for Conservation of Nature and Natural Resources.

UN Environment Programme World Conservation Monitoring Centre (UNEP-WCMC), International Union for Conservation of Nature (IUCN), & National Geographic Society (NGS). (2020). *Protected Planet Report 2020*. Author.

UN Environment Programme World Conservation Monitoring Centre (UNEP-WCMC), & International Union for Conservation of Nature (IUCN). (2024). *Protected Planet: The World Database on Protected Areas (WDPA) and World Database on Other Effective Area-based Conservation Measures (WD-OECM)*. Author.

United Nations Convention on Biological Diversity (UNCBD). (2022). *The final text of the historic Kunming-Montreal Global Biodiversity Framework, agreed at the 15th meeting of the Conference of Parties to the UN Convention on Biological Diversity is now available as document CBD/COP/15/L25*. Author.

Urban, M. C. (2015). Accelerating extinction risk from climate change. *Science*, *348*(6234), 571–573.

Ureta, C., Ramírez-Barrón, M., Sánchez-García, E. A., Cuervo-Robayo, A. P., Munguía-Carrara, M., Mendoza-Ponce, A., Gay, C., & Sánchez-Cordero, V. (2022). Species, taxonomic, and functional group diversities of terrestrial mammals at risk under climate change and land-use/cover change scenarios in Mexico. *Global Change Biology*, *28*(23), 6992–7008.

Visconti, B. P., Butchart, S. H. M., Brooks, T. M., Langhammer, P. F., Marnewick, D., Vergara, S., Yanosky, A., & Watson, J. E. M. (2019). Protected area targets post-2020. *Science*, *364*(6437), 239–241.

Voskamp, A., Fritz, S. A., Köcke, V., Biber, M. F., Nogueira Brockmeyer, T., Bertzky, B., Forrest, M., Goldstein, A., Henderson, S., Hickler, T., Hof, C., Kastner, T., Lang, S., Manning, P., Mascia, M. B., McFadden, I. R., Niamir, A., Noon, M., O'Donnell, B., … Böhning-Gaese, K. (2023). Utilizing multi-objective decision support tools for protected area selection. *One Earth*, *6*(9), 1143–1156.

Wang, F., Zhao, Z., Wang, P., Zhong, L., Yang, S., Tang, J., Hou, S., Tseng, T. H., Cao, Y., & Yang, R. (2024). Over 1/4 of China's terrestrial area significantly contributed both to biodiversity conservation and carbon neutrality, requiring protection. *Science of the Total Environment*, *912*, Article 169070.

Wang, J., Feng, L., Palmer, P. I., Liu, Y., Fang, S., Bösch, H., O'Dell, C. W., Tang, X., Yang, D., Liu, L., & Xia, C. Z. (2020). Large Chinese land carbon sink estimated from atmospheric carbon dioxide data. *Nature*, *586*(7831), 720–723.

Watson, J. E. M., Dudley, N., Segan, D. B., & Hockings, M. (2014). The performance and potential of protected areas. *Nature*, *515*(7525), 67–73.

Watson, J. E. M., Simmonds, J. S., Narain, D., Ward, M., Maron, M., & Maxwell, S. L. (2021). Talk is cheap: Nations must act now to achieve long-term ambitions for biodiversity. *One Earth*, *4*(7), 897–900.

Wu, H., Yu, L., Shen, X., Hua, F., & Ma, K. (2023). Maximizing the potential of protected areas for biodiversity conservation, climate refuge and carbon storage in the face of climate change: A case study of Southwest China. *Biological Conservation*, *284*, Article 110213.

Yang, R., Cao, Y., Hou, S., Peng, Q., Wang, X., Wang, F., Tseng, T. H., Yu, L., Carver, S., Convery, I., Zhao, Z., Shen, X., Li, S., Zheng, Y., Liu, H., Gong, P., & Ma, K. (2020). Cost-effective priorities for the expansion of global terrestrial protected areas: Setting post-2020 global and national targets. *Science Advances*, *6*(37), Article eabc3436.

Yu, L., Du, Z., Dong, R., Zheng, J., Tu, Y., Chen, X., Hao, P., Zhong, B., Peng, D., Zhao, J., Li, X., Yang, J., Fu, H., Yang, G., & Gong, P. (2022). FROM-GLC Plus: Toward near real-time and multi-resolution land cover mapping. *GIScience & Remote Sensing*, *59*(1), 1026–1047.

Zeng, Y., Koh, L. P., & Wilcove, D. S. (2022). Gains in biodiversity conservation and ecosystem services from the expansion of the planet's protected areas. *Science Advances*, *8*(22), Article eabl9885.

Zheng, Q., Ha, T., Prishchepov, A. V., Zeng, Y., Yin, H., & Koh, L. P. (2023). The neglected role of abandoned cropland in supporting both food security and climate change mitigation. *Nature Communications*, *14*(1), Article 6083.

Zhu, L., Hughes, A. C., Zhao, X. Q., Zhou, L. J., Ma, K. P., Shen, X. L., Li, S., Liu, M. Z., Xu, W. B., & Watson, J. E. M. (2021). Regional scalable priorities for national biodiversity and carbon conservation planning in Asia. *Science Advances*, *7*(35), Article eabe4261.

SUPPORTING INFORMATION

Additional supporting information can be found online in the Supporting Information section at the end of this article.